Science of the Total Environment 540 (2016) 444–454

Contents lists available at ScienceDirect

Science of the Total Environment

journal homepage: www.elsevier.com/locate/scitotenv

A high-precision sampling scheme to assess persistence and transport characteristics of micropollutants in rivers

Marc Schwientek [a,b,*], Gaëlle Guillet [b], Hermann Rügner [a,b], Bertram Kuch [c], Peter Grathwohl [b]

[a] Water & Earth System Science (WESS) Competence Cluster c/o University of Tübingen, Hölderlinstr. 12, 72074 Tübingen, Germany
[b] Center of Applied Geoscience, Eberhard Karls University of Tübingen, Hölderlinstr. 12, 72074 Tübingen, Germany
[c] Institute of Sanitary Engineering, Water Quality and Solid Waste Management, University of Stuttgart, Bandtäle 2, 70569 Stuttgart, Germany

HIGHLIGHTS

- Application of extended mass balance approach based on Lagrangian sampling
- Reliable quantification of micropollutants' reactivity in river segments
- Model-aided analyses of measured time series
- Assessment of temporal patterns of removal processes

GRAPHICAL ABSTRACT

ARTICLE INFO

Article history:
Received 30 April 2015
Received in revised form 9 July 2015
Accepted 27 July 2015
Available online 15 August 2015

Keywords:
Micropollutants
River segments
Mass balances
Removal processes
Diurnal patterns

ABSTRACT

Increasing numbers of organic micropollutants are emitted into rivers via municipal wastewaters. Due to their persistence many pollutants pass wastewater treatment plants without substantial removal. Transport and fate of pollutants in receiving waters and export to downstream ecosystems is not well understood. In particular, a better knowledge of processes governing their environmental behavior is needed. Although a lot of data are available concerning the ubiquitous presence of micropollutants in rivers, accurate data on transport and removal rates are lacking. In this paper, a mass balance approach is presented, which is based on the Lagrangian sampling scheme, but extended to account for precise transport velocities and mixing along river stretches. The calculated mass balances allow accurate quantification of pollutants' reactivity along river segments. This is demonstrated for representative members of important groups of micropollutants, e.g. pharmaceuticals, musk fragrances, flame retardants, and pesticides. A model-aided analysis of the measured data series gives insight into the temporal dynamics of removal processes. The occurrence of different removal mechanisms such as photooxidation, microbial degradation, and volatilization is discussed. The results demonstrate, that removal processes are highly variable in time and space and this has to be considered for future studies. The high precision sampling scheme presented could be a powerful tool for quantifying removal processes under different boundary conditions and in river segments with contrasting properties.

1. Introduction

In many parts of the world surface water quality improved significantly during the second half of the 20th century mainly through installation of waste water treatment plants (WWTPs) but also by the development and implementation of additional treatment steps. A novel threat to aquatic ecosystems is posed by the increasing number

* Corresponding author at: Water & Earth System Science (WESS) Competence Cluster c/o University of Tübingen, Hölderlinstr. 12, 72074 Tübingen, Germany.
E-mail address: marc.schwientek@uni-tuebingen.de (M. Schwientek).

http://dx.doi.org/10.1016/j.scitotenv.2015.07.135

and amount of xenobiotics released into the environment (Banjac et al., 2015; Jekel et al., 2015; Ternes, 2007). These 'emerging pollutants', emitted by all of us in everyday life, comprise – among others – pharmaceuticals and personal care products (Carmona et al., 2014; Kasprzyk-Hordern et al., 2009; Ternes et al., 2004), pesticides (Köck-Schulmeyer et al., 2013; Sandstrom et al., 2005), and flame retardants (Meyer and Bester, 2004; Pang et al., 2013). Although mostly emitted via household wastewater and collected by sewer systems, the persistence of many of these compounds in standard waste water treatment processes leads to considerable pollutant loads which are emitted to the receiving waters (Loos et al., 2013; Reemtsma et al., 2006). The efficiency of the treatment process was and still is the subject of many studies (e.g. Bester, 2004; Gómez et al., 2007; Simonich et al., 2002; Ternes, 1998; Yang et al., 2011). However, the fate of micropollutants after their release into the environment is poorly understood and only few data exist concerning environmental removal rates (Köhler and Triebskorn, 2013). Reemtsma et al. (2006) introduced a water cycle spreading index to evaluate the potential of a given substance to accumulate in the water cycle, based on the substance' persistence in the waste water treatment process. It is, however, likely that other or additional elimination processes such as biodegradation during hyporheic exchange, photodegradation or volatilization, occur in flowing waters in particular where milieu conditions foster transformation processes (e.g. von der Ohe et al., 2012). Hence, field investigations are needed to better understand how emerging pollutants behave during environmental transport and how this behavior is controlled by the physico-chemical boundary conditions in rivers. Reliable field data of persistence and transport characteristics of micropollutants in rivers is also a prerequisite for the parameterization of mathematical models which may then be used as prognostic tools.

Assessment of the fate of micropollutants is already difficult under controlled boundary conditions in WWTPs, complicated by transient in- and output fluxes and diurnal patterns of temperature and solar radiation. Majewsky et al. (2013) and Zhang et al. (2008) pointed out that large uncertainties in the evaluation of WWTP performance often arise from too short observation times and the negligence of hydrodynamic effects, leading to inaccurate or even unrealistic (negative) numbers for removal efficiencies. To study such processes in flowing water systems is even more challenging. Inputs from WWTP effluents are typically transient and river segments in which transformation processes of interest occur may comprise long travel distances and/or travel times and varying conditions in terms of river morphology, hydrology and geology.

Methods have been developed to follow distinct water parcels through river segments, and to evaluate reactive processes based on chemical analysis within these water parcels. The largest challenge here is the correct timing of sampling suited to fully encompass a mass of water along its way downstream. This principle is widely termed 'Lagrangian sampling' and was often adopted based on estimates or measurements of flow velocities (Battaglin et al., 2001; Cladière et al., 2014; Moody, 1993; Yu-Chen Lin et al., 2006). Since the effluent flow rates released by WWTPs typically vary within short time periods, concentration changes in the receiving streams are additionally affected by dispersion. Only a sampling scheme capable of capturing these hydrodynamic processes can lead to robust results. One straightforward approach of 'Lagrangian sampling' may be achieved by artificially injecting the micropollutants of interest along with a conservative tracer (Kunkel and Radke, 2011). However, this is usually not compatible with local environmental legislation. A more practicable method for tracking concentration signals of contaminants is based on addition of dye or salt tracers (Barber et al., 2011; Brown et al., 2009; Morrall et al., 2004). The drawback of these methods is that only a snapshot in time is sampled and variations in pollutant transformation processes which occur at time scales beyond the sampling interval (e.g. diurnal cycles) are not captured. Limitations in accuracy may also result if transport properties of the applied tracers differ from those of the investigated pollutants or if the tracer signal is not recovered at a sufficient level as described e.g. by Writer et al. (2012). Some of these problems may be overcome if complete mass balances are determined. The strategy applied by Ahel et al. (1994), who developed the idea of tracking a "large" parcel of water, long enough to include all variability of a 24 hour-cycle, is a suitable approach to further refine the sampling technique and to combine it with state-of-the-art analytical tools and model concepts.

In this study an extended model-aided Lagrangian sampling scheme to assess the fate of contaminants in rivers is developed and tested. The method's potential is demonstrated for representative and widely used members out of the compound groups of pharmaceuticals, polycyclic musk fragrances, phosphorous flame retardants, pesticides, biocides, and bleaching agents. Conclusions regarding dominating attenuation processes and their relevance are drawn.

2. Materials and methods

2.1. Methodological approach

The presented sampling methodology is based on the general idea of the Lagrangian sampling scheme with an enlargement of the investigated water parcel, as adopted by Ahel et al. (1994), and accounting for the conservation of mass at two consecutive cross-sections of a river segment. Water parcels are sampled which are longer than the travel distance to minimize uncertainties due to an inaccurate determination of the travel time and dispersion effects. A quasi-continuous (or high frequency) monitoring of flow rates and concentrations of the river water as it moves through the control cross-sections at the upstream and downstream ends of the selected river segment, respectively, is applied which allows for the determination of pollutant mass balances. The method therefore does not only provide a snapshot of bulk processes but enables the evaluation of transport and transformation mechanisms as a function of time.

Ideally, if the mass flux is subject to diurnal cycles, which is typically the case for wastewater derived contaminants, the monitoring of the enlarged water parcel will cover a whole cycle of 24 h. Subsequently, the analysis of the measured data can be performed for each target compound in terms of a mass balance over the whole sampling period from time t_0 to t_1:

$$\int_{t0}^{t1}\sum_{i=1}^{n}(Q_i\,C_i)_{in}\,dt=\int_{t0+\Delta t}^{t1+\Delta t}(Q\,C)_{out}\,dt+\Delta S \tag{1}$$

where Q_i and C_i denote volumetric water flow rates and compound-specific concentrations entering the river segment via inflows (accounting for possible multiple inflows supplying water and matter to the selected river segment), while Q and C (out) are flow rate and concentrations of the main river at the downstream control cross-section of the segment. Δt is the travel time of the water parcel between the two control cross-sections. ΔS is a bulk sink flux comprising all processes that contribute to a loss of mass within the river segment and is termed "net removal" in later chapters. The relation of ΔS and the total inflow mass into the study segment (= left side of Eq. (1)) is a direct measure for the reactivity (or persistence) of a specific compound along its flow path.

Calculating mass balances according to Eq. (1) requires the following steps: (i) an appropriate river segment has to be identified; the length of which is sufficient to allow detectable transformation processes to occur while the number of inflows has to be low in order to be manageable; diffuse "unknown" gains and losses should be negligible, (ii) the travel time Δt must be determined precisely and (iii) volumetric flow rates and contaminant concentrations of all relevant in- and outflows must be determined quasi-continuously over time.

Furthermore, if Δt is known, continuous measurements of mass fluxes entering and leaving the river segment, shifted by the travel time Δt, can be compared directly. If concentrations vary strongly over time, dispersion along the flow path also has to be considered, e.g. by

use of a suitable modeling tool. The differences of input and output fluxes over time give insight into diurnal patterns of transformation processes.

2.2. Selected river segment

In order to demonstrate the precision of the presented approach a 4 km long segment of the Steinlach River ranging from the central WWTP to the river mouth was selected. The Steinlach River, a 4th order stream, is a tributary of the Neckar River, one of the principal sub-catchments of the Rhine Basin in Southwest Germany (Fig. 1). It has a total length of 25 km and drains a hilly catchment in the northern foreland of the Swabian Alb mountains with an area of 140 km^2, collecting a mean discharge (Q) of 1.7 $m^3\ s^{-1}$ (http://www.hvz.baden-wuerttemberg.de/). Mean annual air temperature is approximately 8 °C (City of Tübingen) and areal precipitation is 900 mm yr^{-1} (1980–2009) with a slight maximum during the summer months. Land-use is dominated by a mix of rain-fed agriculture (49%) and forest (39%). The population density is approximately 340 inhabitants per km^2. The wastewater of the approximately 50,000 inhabitants is treated in the central WWTP located 4 km from the catchment outlet. Including industrial and commercial waste waters it treats an inhabitant equivalent of 99,000 and is equipped with a secondary and tertiary treatment stage, largely eliminating nitrate and phosphorous loads biologically. The mean effluent flow rate is 260 $l\ s^{-1}$ and is released at the right bank of the river closely upstream of the selected river segment. Upstream of the WWTP the Steinlach River receives wastewater only during intense precipitation events when the combined sewer system may overflow. Downstream of the WWTP the water of the Steinlach River consists of ca. 15% treated wastewater during mean discharge conditions, but the proportion may rise well above 50% after long dry weather periods. Along the studied 4 km river stretch the Steinlach River flows mainly in a straightened channel through the southern suburbs of the City of Tübingen and receives only minor tributaries (Fig. 1). Of note is a constructed diversion (the Mühlbach) which derives water from the main stem about a kilometer downstream of the WWTP effluent which flows directly into the Neckar River. The river bed is mostly permeable consisting of medium sized gravel to larger cobbles. The mean slope is 7‰, enhancing hyporheic exchange where possible. The mean width of the channel is approximately 8 m with little variation. The mean water depth on the day of sampling was calculated from the surface of the water body (ca. 35,000 m^2) and the mobile water volume (ca. 8200 m^3 = discharge × travel time) to be approximately 0.25 m. The water was clear with concentrations of suspended matter below 3 mg l^{-1}. Shading of the river channel is sparse, so solar radiation can mostly penetrate the water body directly.

2.3. Determination of travel time Δt

Δt was determined experimentally using the electrical conductivity signal (EC) emitted by the WWTP as an environmental tracer. Due to the varying use of water in the households during the day, effluent flow rates of WWTPs typically show a diurnal pattern. Provided that the EC in the effluent and the river water differs sufficiently and the effluent flow rates are not too small in relation to the river's discharge (which is the case for the Steinlach River), these variations are reflected in similar patterns of EC in river water downstream of the WWTP. Using CTD divers (Schlumberger Water Sciences Technology, Canada) these patterns were measured continuously at the upper and lower control cross-sections of the river segment during variable discharge conditions. Δt was determined directly as the time shift between paired signals of pronounced peaks which occur in both time series.

Underlying assumptions are that EC behaves conservatively and that the peak travel times are not substantially affected by dispersion. The determined travel times were related to the respective discharges (taken from the gauging station in the middle part of the studied river segment) and an empirical function could be fitted describing Δt as a function of Q (Fig. 2).

2.4. Lagrangian sampling and determination of mass fluxes

Sampling and on-line measurements were conducted from July 2 to 3, 2013. Conditions were sunny with air temperatures up to 28 °C, thus intense solar radiation and no rainfall. After a dry weather period Q in the rivers was low.

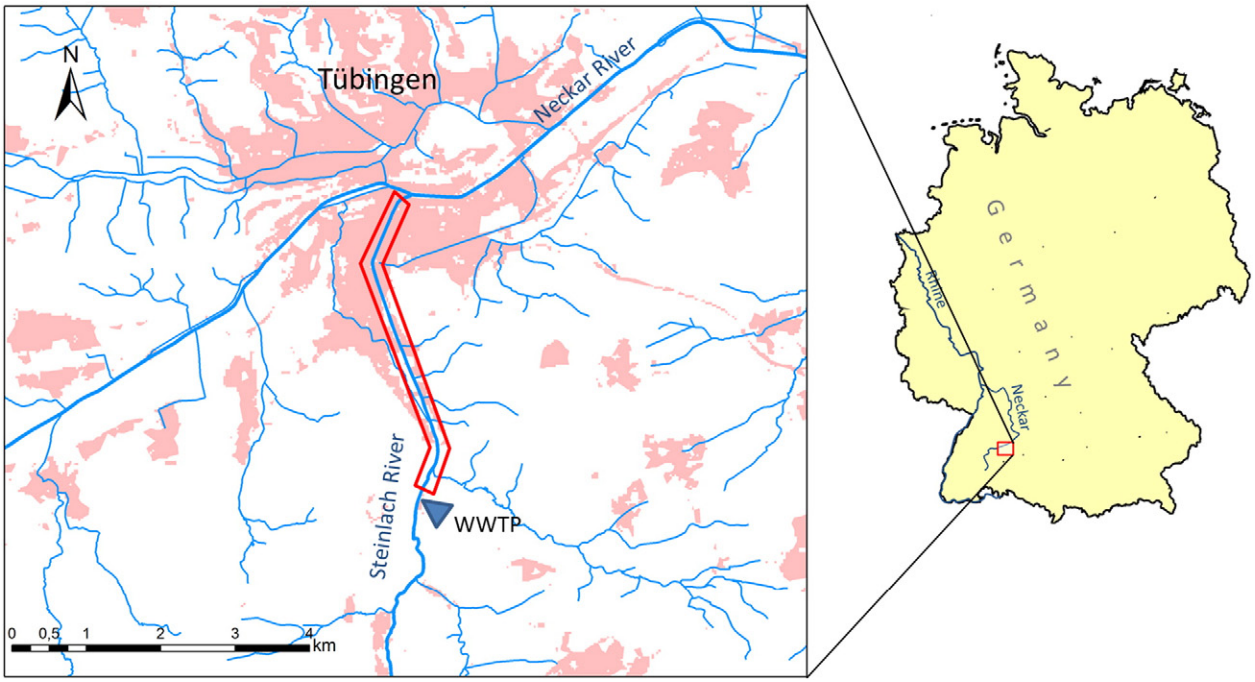

Fig. 1. Selected river segment along the lower Steinlach River between the outlet of the catchment's wastewater treatment plant (WWTP) and the confluence with the Neckar River.

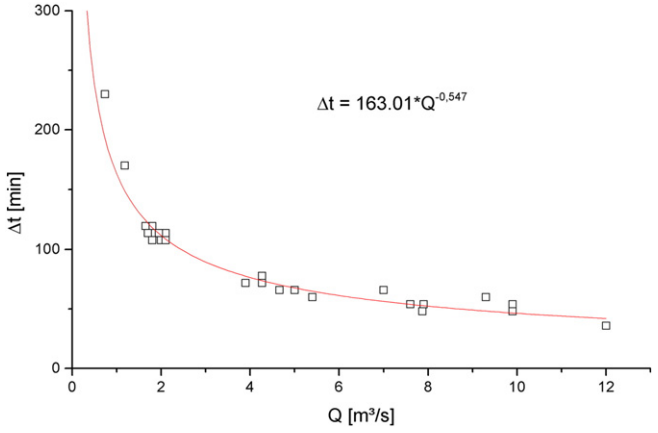

Fig. 2. Empirical function describing the relation between the water travel time Δ*t* and *discharge Q* along the selected river segment.

2.4.1. Sampling in the Steinlach River

Sampling of the Steinlach River was conducted using automated samplers (ISCO 3700, Teledyne Isco, Inc., USA) which were placed at the upper and lower control cross-sections, respectively. The upstream location was situated approximately 100 m downstream from the WWTP outfall. This distance was sufficient to provide complete mixing of treated wastewater within the river cross-section (see Section 2.6) which was checked repeatedly by measurement of lateral EC profiles and by grab samples across the river width. The downstream sampler was placed 100 m upstream the river mouth in the City of Tübingen. The inlets of the samplers were placed in the middle of the river. Both samplers were equipped with teflon tubing and 1 l glass bottles. Samples were taken every 15 min and composite samples of 3.6 l representing 2 h intervals were mixed when the samplers were emptied every 6 h. This ensured sample volumes sufficient for all analytical procedures and kept the number of samples manageable. The sampling program of the upstream sampler started at 06:00 in the morning and ended at 05:45 on the next day, the downstream sampler started with a time shift of 3 h according to the water travel time determined from the $\Delta t - Q$ relationship. In total, 35 samples were collected (including tributaries, Section 2.4.2).

For the determination of *Q* of the Steinlach River at the upper control cross-section continuous water level data (time interval 5 min) was used from an existing measuring station located 200 m upstream of the WWTP (see Fig. 3). The water levels were converted to *Q* by means of an existing rating curve which was checked repeatedly. EC was used as a tracer to calculate the flow rates supplied by the WWTP

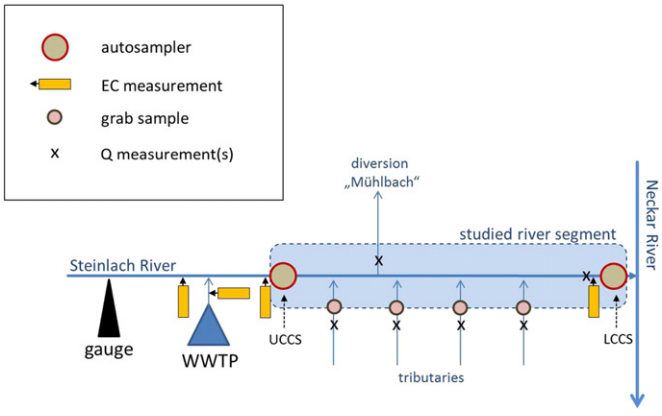

Fig. 3. Conceptual diagram showing all measurement and sampling locations and the studied segment of the Steinlach River. UCCS = upper control cross-section, LCCS = lower control cross-section.

and the total discharge (Q_{tot}) passing the upper control-cross section of the river segment: EC data were measured at 5 min intervals (1) in the Steinlach River upstream of the WWTP effluent, (2) in the WWTP effluent, and (3) at the location of the upper control cross-section (downstream of the WWTP effluent) using CTD divers (Schlumberger Water Sciences Technology, Canada). Using a two-component mixing equation, the flow rate of the WWTP effluent could be calculated as follows:

$$Q_{ef} = Q_g \times \frac{EC3 - EC1}{EC2 - EC3} \quad (2)$$

where Q_{ef} and Q_g are the flow rates of the WWTP effluent and the gauged discharge measured at the upstream station respectively, and *EC1*, *EC2*, and *EC3* are the electrical conductivities measured at locations (1), (2), and (3) respectively. Q_{tot} may then be computed as the sum of Q_{ef} and Q_g. A schematic map of all measurement and sampling locations is given in Fig. 3.

At the lower control cross-section *Q* had to be calculated. As a first step, all *Q* values flowing into the river section were balanced to generate a total input signal. The routing of the input *Q* through the 4 km river channel was modeled by the convolution of a dispersive distribution function (Maloszewski and Zuber, 1982; Maloszewski, 1993). Required parameters are the mean travel time of the Q signal and the dispersion parameter. The mean travel time of the Q signal is not identical with the water travel time Δt, but can be described by the kinematic wave approach. Assuming that Q and water depth are related according to the Manning equation, the wave velocity is 5/3 times the mean water flow velocity (e.g. Dingman, 1984). Hence, the mean travel time of the wave is 3/5 times Δt. The dispersion parameter and the mean travel time were derived from fitting the dispersion model to the measured EC time series (for further details see Section 2.7), assuming that the dispersion affecting the transport of matter and the propagation of a wave are similar. Additionally, Q at the lower control cross-section was measured twice during the sampling campaign and the results fitted well to the modeled hydrograph (deviations from the modeled Q of 4 and 5%, respectively).

2.4.2. Tributaries

The tributaries are not affected by wastewaters and the total contribution of discharge to the Steinlach River was no more than approximately 2%. Thus, concentrations and discharges were considered constant. Concentrations in the tributaries were determined in a single grab-sample per tributary during the 24 h campaign. Q was measured once in the largest tributary (Ehrenbach), entering the Steinlach River from the right hand side closely to the upper control cross-section (Fig. 1), using a flow meter (Ott C2, Kempten, Germany). The flow rates of the three remaining tributaries could not be measured with a flow meter, since water depths were <2 cm. They were estimated during sampling which can be considered sufficient as each tributary supplied only roughly 1‰ of the total Q.

2.4.3. Determination of mass fluxes

Mass fluxes are given by the product of the volumetric water flow rate and the concentration of the compound of interest. Identified inflows into the river segment in the sense of Eq. (1) were the Steinlach River itself entering the segment at the upper control cross-section and the four tributaries supplying water during the period of sampling from July 2–3, 2013, i.e. mass fluxes of the tributaries were treated as if they entered the study river segment at the upstream end. The only outflow from the river segment was the Steinlach at the lower control cross-section close to its confluence with the Neckar River. For the Mühlbach (see above) it was assumed that the water chemistry of the diverted water was identical with the water entering the river segment. Thus, for the mass balance, the input Q into the studied segment was reduced by the constant flow rate of the Mühlbach (53 l s^{-1}). This

assumption could potentially lead to a slight underestimation of removal processes.

2.5. Analyzed compounds

2.5.1. Selection of analytes

The selection of investigated micropollutants followed criteria such as different kinds of usage and input patterns (e.g. pharmaceuticals, industrial chemicals, personal care products and pesticides, see Table 1), permanent occurrence in the municipal wastewater, and different physico-chemical properties. The latter determine transport behavior (water dissolved, particle-associated) and elimination mechanisms (sorption, volatilization, chemical or biological degradation) of the substances in the rivers. For example, the anticonvulsant carbamazepine behaves relatively conservative (transport in the water phase, low degradability) and was proposed as a persistent marker tracing the pathways of treated sewage (Clara et al., 2004; Glassmeyer et al., 2005; Nakada et al., 2008). The synthetic musks HHCB (galaxolide, 1,3,4,6,7,8-hexahydro-4,6,6,7,8,8-hexamethylcyclopenta-g-2-benzopyran) and AHTN (Tonalide, 7-Acetyl-1,1,3,4,4,6-hexamethyl-1,2,3,4-tetrahydronaphthalene) were characterized by a pronounced seasonality in surface water due to their temperature-dependent attenuation in WWTPs (Musolff et al., 2009). Additionally, sediment/water distribution coefficients of the synthetic musks indicate a distinct sorption tendency of these substances and thus sorption may be considered as an important process for the fate of these compounds in the environment (EPA, 2014). In comparison to that tetraacetyldiamine (TAED) shows less sorption (HERA, 2002), but the substance used as bleaching activator in detergents is easily biodegradable. The flame retardants TCEP (tris-(2-chloroethyl)-phosphate), TCPP (tris-(2-chloro, 1-methylethyl)-phosphate) and TDCPP (tris(1,3-dichloro-2-propyl) phosphate) are frequently used in polymers and foams and thus may reach the aquatic environment not only by discharge of wastewater, but also by other diffuse sources (Regnery and Püttmann, 2010a,b).

2.5.2. Analytical procedures

Collected samples were shipped within 24 h to the laboratory at the Institute of Sanitary Engineering, University of Stuttgart, for the analysis of organic micropollutants. The tested compound groups and representative target substances are given in Table 1.

2.5.2.1. Sample preparation for diclofenac, naproxen and triclosan. After adding the internal standards diclofenac-d4 (50 μL, 4 ng μL^{-1} in dichloromethane), naproxen-d3 (50 μL, 4 ng μL^{-1} in dichloromethane), mecoprop-d3 (20 μL, 1 ng μL^{-1} in methanol) and triclosan-d3 (50 μL, 1 ng μL^{-1} in methanol) the pH-value of the non-filtered water samples (2 L) was adjusted to pH 2.5 using sulfuric acid (96%). The analytes were extracted via liquid/liquid-extraction (dichloromethane, 2 × 80 mL). The combined organic phases were rotavaporated to approximately 2 mL and dried with sodium sulfate. Prior to GC/MS-analysis the extracts were concentrated with a nitrogen stream (40 °C) to dryness and re-dissolved in a solution of the derivatization agent TMSH (20 μL trimethylsufoniumhydroxide, 0.25 M in methanol).

2.5.2.2. Sample preparation for other organic compounds. The non-filtered water sample (2 L) was spiked with internal standards (100 μL AHTN-d3, 1 ng μL^{-1} in dichloromethane; 50 μL carbamazepine-d10, 2 ng μL^{-1} in dichloromethane; 100 μL PAH-standard containing 16 perdeuterated PAHs according to US-EPA, each compound 1 ng mL^{-1} in toluene). Liquid/liquid extraction with dichloromethane and further steps were performed as described above. Prior to GC/MS-analysis the extracts were concentrated in a nitrogen stream at 25 °C to a volume of 50 μL.

2.5.2.3. GC/MS-analysis. GC/MS-analysis was performed on a high resolution gas chromatograph Agilent 6890 directly coupled with a low resolution mass selective detector Agilent 5975. The analytes were quantified directly via the isotope dilution method or external calibration with internal standards. Due to the large sample volumes and the enrichment factors (>1:40,000) limits of quantification were in the range of 1 ng L^{-1}.

In parallel, an aliquot of each sample was transferred to the laboratory at the Center for Applied Geoscience, University of Tübingen, for the analysis of major ions and DOC. Prior to measurement the samples were filtered through 0.45 μm cellulose-acetate filters. Ion concentrations were measured using an ion chromatograph (DX 500, DIONEX). DOC was determined after acidification to pH 2 and purging with nitrogen gas using a TOC analyzer (Elementar HighTOC; thermal oxidation at 680 °C and CO_2 quantification using an IR detector). Multiple analyses of laboratory standards yielded an analytical uncertainty of less than ±5%.

2.6. Quality control of sampling and chemical analyses

To ensure complete mixing of river water and treated waste water at the upper control cross-section, lateral EC profiles were measured across the section. On average, EC in treated wastewater was 95% elevated in relation to river water at the time of sampling, yet the coefficient of variation (COV; 8 measurements) for EC in the cross-section was only 0.4%. Thus, complete mixing was assumed. In addition, grab samples were taken simultaneously close to both river banks and at the inlet of the automated sampler tubing in the middle of the river. For these samples the coefficient of variation (COV; 3 samples) was also calculated and interpreted in terms of reproducibility of the lab analysis.

Table 1
Micropollutants and their octanol/water partitioning coefficients.

Group	Compound	Log K_{ow} (pH 6 to 8)	Source
Pharmaceuticals	Carbamazepine	2.67 (pH = 7.5)	Scheytt et al. (2005)
	Oxcarbazepine	1.11	http://www.chemspider.com/
	Diclofenac	1.9 (pH = 7)	Scheytt et al. (2005)
	Naproxen	1.18 (pH = 7.4–8.1)	de Ridder et al. (2011)
Polycyclic musk fragrances	HHCB	5.3	Balk and Ford (1999)
	HHCB-lactone	4.7	Chen et al. (2009)
	AHTN	5.7	Balk and Ford (1999)
	OTNE	5.7	Chen et al. (2009)
Phosphorus flame retardants	TCPP	2.59	WHO (1998)
	TDCPP/TDCP	3.8	WHO (1998)
	TCEP	1.43	Sasaki et al. (1981)
Pesticides/insect repellents	Mecoprop	−0.12 (pH = 7)	Ilchmann et al. (1993)
	DEET	2.02 (pH = 6.6)	Moody et al. (1987)
Biocides	Triclosan	4.31 (pH = 7.9)	Matamoros et al. (2012)
Bleaching agents	TAED	0.09	Deluchat et al. (2002)

2.7. Model aided data analysis

In contrast to the balancing of bulk pollutant mass fluxes over 24 h according to Eq. (1), input and output mass fluxes as a function of time at the upper and lower control cross-sections respectively, were compared using a lumped parameter model. In this context the effects of dispersion and mixing with neighboring water parcels – as implied in the original Lagrangian sampling concept – are then no more negligible. The applied approach transforms an input time series into an output signal by convoluting the input with a transit time distribution function (e.g. McGuire and McDonnell, 2006):

$$C_{out}(t) = \int_0^t C_{in}(t-\tau)g(\tau)d\tau \quad (3)$$

where $C_{out}(t)$ and $C_{in}(t)$ are the output and input tracer concentrations measured as a function of time, respectively, $g(\tau)$ is the transit time distribution function of the tracer particles in the system under investigation, and τ is the transit time of a single tracer particle through the system. As a transit time distribution function representing advection and dispersion processes in the river channel, the dispersion model was chosen (for details see e.g. Maloszewski and Zuber, 1982; Maloszewski, 1993). Here, the transit time distribution is defined by the following function:

$$g(\tau) = \frac{1}{\tau\sqrt{\frac{4\pi P_D \tau}{\Delta T}}} \exp\left[-\frac{\left(1-\frac{\tau}{\Delta T}\right)^2}{\frac{4P_D\tau}{\Delta T}}\right]. \quad (4)$$

To infer the accurate mean transit time ΔT and the dispersion parameter P_D, EC was used as a conservative tracer. The flow-weighted input function $C_{in}(t)$ was calculated from the EC, measured at 5 min intervals in water of the Steinlach River at the upper control cross-section, and of the four tributaries (single measurements). The model output $C_{out}(t)$ was fitted to the EC time series measured in the Steinlach River at the lower control cross-section. The fitted model was then applied to the compounds of interest accordingly. In the case of the modeled micropollutants and ions, the input time series had to be extended backwards by a dummy value to minimize artifacts influencing the modeled concentrations of the first time step. As a dummy, the first input concentration was used twice in a row. Differences between the modeled output and the concentrations measured could be assigned to transformation processes since the model only combines the effects of advection and dispersion but does not include reactive transport.

3. Results and discussion

3.1. Detected concentrations

A summary of the average concentrations of organic micropollutants and ions and the observed concentration ranges at the upper and lower control cross-sections as well as the concentrations measured in the tributaries is given in Table 2. Additionally, the total input and output mass fluxes over 24 h are shown. Maximum concentrations were measured for diclofenac ranging to almost 500 ng L^{-1} at the upper control cross-section. Similarly, high concentrations were encountered for HHCB-lactone. Concentrations of the parent compound HHCB did not exceed 100 ng L^{-1} even close to the outfall of the WWTP, indicating that oxidation of HHCB occurred in the treatment process (Bester, 2004). The concentrations, in particular at the upper control cross-section, are mainly defined by the dilution of the discharged treated wastewater in the receiving water as under dry weather conditions the entry of wastewater-related micropollutants into the system via combined sewer overflows (CSO) is negligible. On average, treated wastewater contributed 28% to the total stream flow. Hence, concentrations of compounds that exclusively derive from wastewater can be estimated to be at least three times higher in the effluent. Micropollutant concentrations in the tributaries were usually low or below detection limit, which indicates that the main source of all analyzed compounds is treated wastewater.

The remarkably large concentration changes observed in the Steinlach River with minima far below the average values are the result of a 1.5 h maintenance period at the WWTP which was not announced. During that time no effluent was discharged into the river (visible also in the EC time series, see Fig. 5). Two composite samples were affected by the resulting lower concentrations. The "gap" in the time series of concentrations was less pronounced at the lower control cross-section due to smoothing by dispersion.

Ions with the highest concentrations (Table 2) were calcium (Ca^{2+}) and sulfate (SO_4^{2-}) representing the geogenic background of the catchment with a high proportion of carbonate rocks. The strongest relative change due to the maintenance of the WWTP was observed for potassium (K^+) and sodium (Na^+), followed by nitrate (NO_3^-) and chloride (Cl^-), which emphasizes the conclusion that these ions derive from wastewater to a large extent. Tributaries not affected by wastewaters contain much lower concentrations of these compounds. The relatively high concentrations of NO_3^- in tributaries 1 and 3 presumably derive from arable land present in the catchments. Tributaries 2–4 are increasingly influenced by local marl geology which is the presumed source of the relatively high Mg^{2+} concentrations compared to the Steinlach River.

Reproducibility of measured concentrations for triplicate samples (independently sampled at the same time; COV: coefficient of variation, see Section 2.6) are given in Table 3. For most compounds reproducibility was good, as indicated by COV values which were generally in the range below 2% and never exceeded 4% for micropollutants and even better for major ions.

3.2. Mass balances

Mass balances and the net removal ΔS were calculated for the micropollutants and major ions according to Eq. (1). The results are displayed in Table 2. For an evaluation of the efficiency of transformation processes, ΔS is related to the total input mass flux. The resulting relative net removals for the single compounds are depicted in Fig. 4. The very low calculated net removal for the conservative ions Na^+, SO_4^{2-}, and Cl^- ($-0.1\% < \Delta S > 0.3\%$) may be interpreted as indicators for the high accuracy of the technical procedures involved in balancing mass fluxes (including analytical errors). Analysis of organic micropollutants is typically associated with larger uncertainties. However, the COV values for organics given in Table 3 (standard deviations of < 4%) justify that these mass balances are also deemed very reliable.

According to the computed relative net removals, the most reactive substances were oxcarbazepine and OTNE with net removals of 50% or above. An intermediate removal rate was observed for the compounds triclosan, HHCB, AHTN, TAED, HHCB-lactone, and diclofenac with net removals between 17 and 37%. Small removals, e.g. 1 to 10% for TDCPP, carbamazepine, mecoprop, and TCEP have to be interpreted with some caution since the uncertainties of the procedures involved might not be negligible in these cases, in particular where pollutant concentration were very low. The pharmaceutical carbamazepine and the chlorinated flame retardants TCEP, TDCPP, and TCPP have been described to be persistent by other studies (Löffler et al., 2005; Meyer and Bester, 2004). This is in good agreement with the results presented here which show removals close to 0% for these compounds.

As mentioned above, Na^+, SO_4^{2-}, and Cl^- are usually considered conservative. Accordingly, the mass balances for these ions are almost perfectly closed with net removals close to zero. NO_3^-, one of the most reactive nitrogen species, may be consumed by denitrification and plant uptake (Birgand et al., 2007). The determined net removal of 4.2% appears reasonable given the short travel time in relation to the

Table 2
Discharge (*Q*), pH, EC and micropollutant and major ion concentrations measured at the upper (UCCS) and lower (LCCS) control cross-sections and in tributaries, as well as respective total input and output mass fluxes.

					pharmaceuticals				polycyclic musk fragrances				phosphorous flame retardants			pesticides/insect repellents		biocides	bleaching agents
concentrations		Q [$m^3\ s^{-1}$]	pH	EC [µS/cm]	carbamazepine [ng l^{-1}]	oxcarbazepine [ng l^{-1}]	diclofenac [ng l^{-1}]	naproxen [ng l^{-1}]	OTNE [ng l^{-1}]	HHCB [ng l^{-1}]	HHCB-lactone [ng l^{-1}]	AHTN [ng l^{-1}]	TCEP [ng l^{-1}]	TCPP [ng l^{-1}]	TDCPP [ng l^{-1}]	mecoprop [ng l^{-1}]	DEET [ng l^{-1}]	triclosan [ng l^{-1}]	TAED [ng l^{-1}]
location																			
UCCS	*average*	0,594	8,0	722	133	46	367	65	142	72	331	12	64	149	39	26	62	21	11
	range	(0.50-0.73)	(7.6-8.2)	(608-759)	(35-172)	(5-86)	(82-482)	(23-85)	(49-186)	(26-95)	(108-404)	(5-15)	(37-90)	(41-211)	(12-48)	(14-36)	(18-83)	(15-25)	(3-20)
tributary 1		0.013	8.3	775	1.3	b.d.l.	b.d.l.	b.d.l.	9	6	18	2	19	4	2	b.d.l.	0,9	b.d.l.	5
tributary 2		0.001	8.2	712	0.9	b.d.l.	b.d.l.	b.d.l.	6	2	10	1	10	1.5	3	b.d.l.	1,4	b.d.l.	b.d.l.
tributary 3		0.001	8.1	803	1.3	b.d.l.	b.d.l.	b.d.l.	2	2	12	3	29	3	6	b.d.l.	1,5	5	b.d.l.
tributary 4		0.001	8.1	881	b.d.l.	b.d.l.	b.d.l.	b.d.l.	18	11	22	5	38	4	5	b.d.l.	2	5	b.d.l.
LCCS	*average*	0.610	8.4	718	127	18	302	57	74	49	266	9	58	151	38	24	62	13	9
	range	(0.51-0.69)	(8.2-8.6)	(649-757)	(65-163)	(5-37)	(112-419)	(27-78)	(27-118)	(27-71)	(168-326)	(5-13)	(35-72)	(97-194)	(29-44)	(17-34)	(38-85)	(6-21)	(4-18)
total mass fluxes					[g d^{-1}]	[g d^{-1}]	[g d^{-1}]	[g d^{-1}]	[g d^{-1}]	[g d^{-1}]	[g d^{-1}]	[g d^{-1}]	[g d^{-1}]	[g d^{-1}]	[g d^{-1}]	[g d^{-1}]	[g d^{-1}]	[g d^{-1}]	[g d^{-1}]
Input					7.02	2.40	19.57	3.45	7.37	3.69	17.33	0.61	3.47	7.92	2.03	1.40	3.31	1.08	0,62
Output					6.83	0.96	16.21	3.07	3.72	2.49	14.24	0.46	3.11	8.13	2.01	1.27	3.34	0.67	0.50

Table 2 (*continued*)

concentrations		Na^+ [mg l^{-1}]	K^+ [mg l^{-1}]	Ca^{2+} [mg l^{-1}]	Mg^{2+} [mg l^{-1}]	NO_3^- [mg l^{-1}]	Cl^- [mg l^{-1}]	SO_4^{2-} [mg l^{-1}]
location								
UCCS	*average*	38.8	6.1	105.3	10.0	19.6	53.9	65.8
	range	(23.1-44.4)	(3.2-7.2)	(93.9-107.5)	(9.0-10.6)	(12.6-23.1)	(35.8-59.5)	(57.1-69.0)
tributary 1		24.5	2.6	92.2	26.9	14.6	29.3	92.0
tributary 2		22.5	2.6	59.6	43.8	3.0	10.0	63.8
tributary 3		19.7	3.5	55.9	59.2	12.2	7.4	21.7
tributary 4		14.1	2.0	91.7	50.0	9.8	44.6	18.9
LCCS	*average*	38.5	6.1	105.6	12.2	18.6	53.5	66.4
	range	(29.2-43.7)	(4.4-7.1)	(98.3-108.6)	(11.8-12.6)	(14.1-22.0)	(42.9-59.0)	(61.8-69.5)
total mass fluxes		[kg d^{-1}]	[kg d^{-1}]	[kg d^{-1}]	[kg d^{-1}]	[kg d^{-1}]	[kg d^{-1}]	[kg d^{-1}]
Input		2056	325	5563	560	1044	2842	3538
Output		2047	323	5591	647	999	2840	3531

b.d.l.: below detection limit.
n.a. not applicable.

Table 3
Analyzed compounds (+major ions) and analytical reproducibility of measured concentrations for triplicate samples (COV: coefficient of variation).

Compound	COV	Compound	COV
Carbamazepine	0.7%	OTNE	1.4%
Oxcarbazepine	0.1%	HHCB	1.3%
Diclofenac	1.1%	HHCB – Lactone	1.0%
Naproxen	2.1%	AHTN	1.0%
Mecoprop	1.9%	Na	1.1%
DEET	2.0%	K^+	1.5%
TCEP	2.8%	Ca^{2+}	0.6%
TCPP	0.3%	Mg^{2+}	1.1%
TDCPP	2.4%	NO_3^-	0.9%
Triclosan	1.0%	Cl^-	0.7%
TAED	4.0%	SO_4^{2-}	0.1%

relatively large water volume to be processed. On the other hand, this number gives an impression of the fast transformation that the most reactive organic compounds undergo. For Mg^{2+} (−16%) the mass balance did not work out which is likely a matter of an unidentified input. Increasing concentrations of Mg^{2+} along the studied river segment have repeatedly been encountered which cannot be explained by known sources. A geochemical reaction such as dolomite dissolution is possible. For Ca^{2+} a similar effect was not observed, however, this may probably be masked by its tenfold-higher concentrations.

3.3. Temporal dynamics of the removal processes

The fitting of the dispersion model to measured EC data at the lower control cross-section (Fig. 5) revealed a travel time of the water of 225 min (compared to 204 min determined according to the Δt — Q-relationship; Fig. 2).

Comparison of modeled and measured EC at the lower control cross-section revealed a good fit. The reason for the observed differences between 12:00 and 18:00 remains unclear. During reduced wastewater discharge resulting from maintenance works at the WWTP the modeled and measured data are slightly shifted. Reasons for that might be hydrodynamic effects since the discharge decreased during that period whereas steady-state conditions are assumed in the dispersion model. Moreover, also water chemistry changed, triggering ion exchange processes between water and river bed and leading to retardation. After steady state flow conditions had re-stabilized, the model and data fit reasonably well again.

Fig. 6 shows observed vs. modeled diurnal concentration patterns for the pharmaceuticals carbamazepine and oxcarbazepine and the musk fragrance AHTN; these compounds could be seen as representatives of the three characteristic types of reactive transport encountered during the current study. The micropollutants' concentrations were predicted using the model parameters found by fitting EC. Since the model only comprises the effects of advection and dispersion, any transformation processes along the river segment are expected to result in an overestimation of the measured concentrations. For carbamazepine, the observed and modeled curves are very similar throughout the day, which reflects the conservative behavior of this compound. The small deviations of the curves may be the result of "boundary effects" at the beginning of the model period (i.e. influence of preceding water parcels) and of composite sampling during the concentration decrease due to WWTP maintenance.

In comparison, AHTN shows a net removal during the daytime period of the sampling campaign particularly between 13:00 and 23:00. Removal is apparently close to zero around the time with no input due to WWTP maintenance (21:00). However, net release from transient storages in the river channel (e.g. stagnant zones) and hyporheic zone (mixing zone of surface and groundwater below the river bed) during this time period of steeply decreasing concentrations in river water could mask any transformation processes (compare also "too high" concentration of carbamazepine at that time). Additionally, the relatively high octanol–water partitioning coefficient (log K_{OW} = 5.7 according to Balk and Ford, 1999) and thus sorption tendency of AHTN may support sorption/desorption effects. Fast desorption from outer parts of small particles may sustain a considerable concentration in river water.

As opposed to daytime the modeled and observed AHTN concentrations are very close after midnight. An obvious interpretation of that pattern could be the occurrence of photochemical reactions: The weather conditions were sunny during the whole day and the solar radiation was most intense around 13:00 (noon + 1 h during summer time). A water parcel which started at 11:10 at the upper control cross-section and arrived at 14:50 at the lower control cross-section (according to the measured travel time) would have experienced the maximum sum of solar energy input. This is in line with the maximum "loss" of AHTN around 15:00 as shown in Fig. 6. Photodegradation has been reported for AHTN (e.g. Bester, 2005; Buerge et al., 2003).

Andreozzi et al. (2002) have shown that photochemical reactions may be further enhanced by the occurrence of nitrate due to the formation of OH^- radicals. Also, the presence of humic substances may influence photodegradability. However, converse effects have been reported

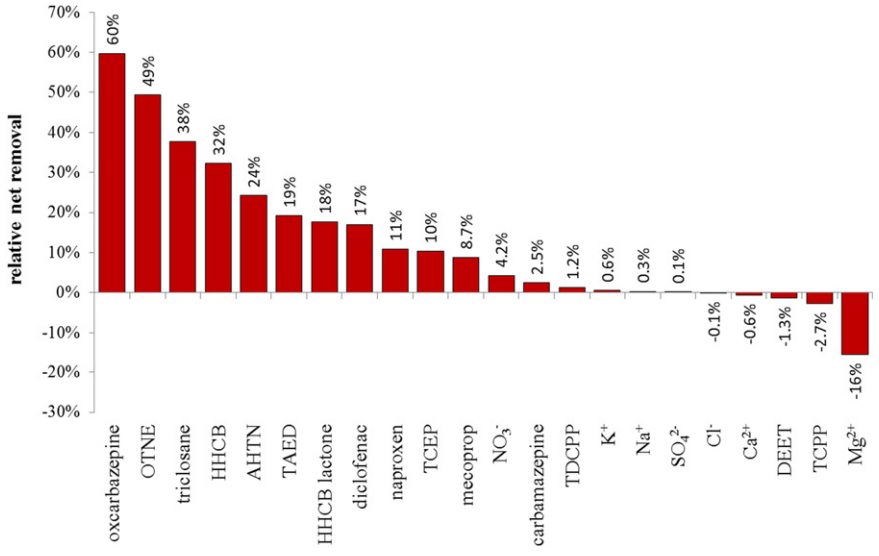

Fig. 4. Calculated relative net removals along the studied river segment for various compounds.

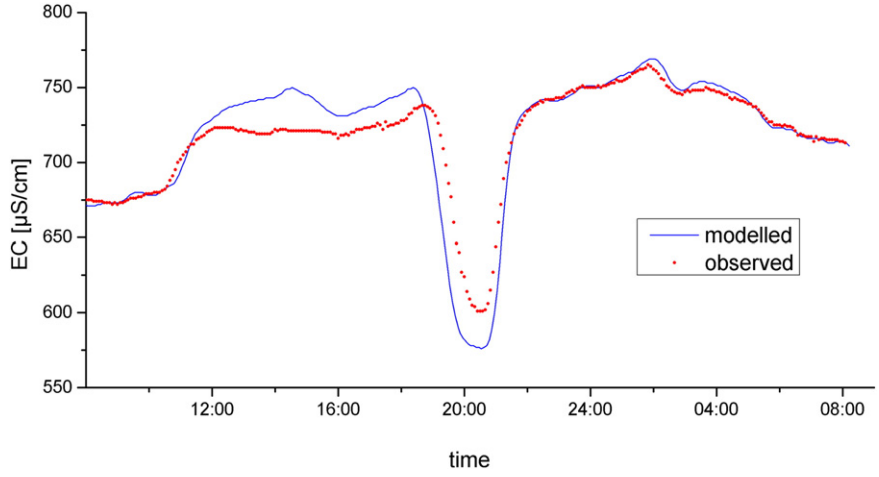

Fig. 5. EC time series measured in the Steinlach River at the LCCS and modeled using the dispersion model ($P_D = 0.002$, goodness of fit SIGMA = 0.9 µS/cm).

(Andreozzi et al., 2002; Lester et al., 2013). The mean DOC concentrations in the Steinlach during sampling were 3.5 mg L^{-1} at the upper and 3.4 mg L^{-1} at the lower control cross-section, respectively. The importance thereof for any photochemical reactions is not clear and requires further research. AHTN (and other musk fragrances such as OTNE and HHCB) may also be subjected to volatilization, which would also be more pronounced at elevated temperatures during day time (see discussion below). These two processes are proposed as the main removal mechanisms affecting AHTN in the studied river segment

A third kind of pattern is observed for oxcarbazepine. This constituent displays an evolution which is similar to AHTN in that removal is apparently maximal in the afternoon hours. In contrast to AHTN, however, a considerable net removal is still observable during nighttime. Besides an obvious light-dependency of distinct removal processes, there is at least one additional transformation mechanism which is still active during night. Relevant for biodegradation and volatilization is the average temperature of the water parcel during its travel time. This was calculated based on continuously measured temperatures at the upper and the lower control cross-sections, shifted by the determined travel time of 225 min. The averaged temperatures in water parcels arriving at the lower control cross-section are shown in Fig. 7 and were highest at 16:00 (17.9 °C) and lowest at 7:45 (15.4 °C). Hence, the diurnal temperature cycle is only partly in phase with the bulk intensity of the observed transformation processes. This fact once again indicates a superposition of different independent transformation mechanisms.

While photo-oxidation of AHTN is a likely mechanism, HHCB is only weakly photodegradable (Buerge et al., 2003). Yet, the bulk removal of 32% determined by the mass balance of HHCB is important. According to Zhang et al. (2013) the presence of HHCB-lactone indicates the biodegradation of HHCB. Concentrations of HHCB-lactone were already high at the upper control cross-section (Table 2). Any further degradation in the river should be reflected by increases of the concentration ratio HHCB-lactone/HHCB. This ratio was modeled for the lower control cross-section as described before. The result is shown in Fig. 7. An increase of the ratio along the river segment indicates transformation of HHCB, likely to HHCB-lactone. As before, the intensity of this transformation is displayed by the departure of modeled and observed curves. This modeled pattern shows a maximum intensity of biodegradation of HHCB during the late afternoon hours. The process intensity coincides fairly well with the pattern of the average water parcel temperature (Fig. 7). The dependency of the HHCB-lactone/HHCB ratio on surface water temperature was also shown for the adjacent catchment of the

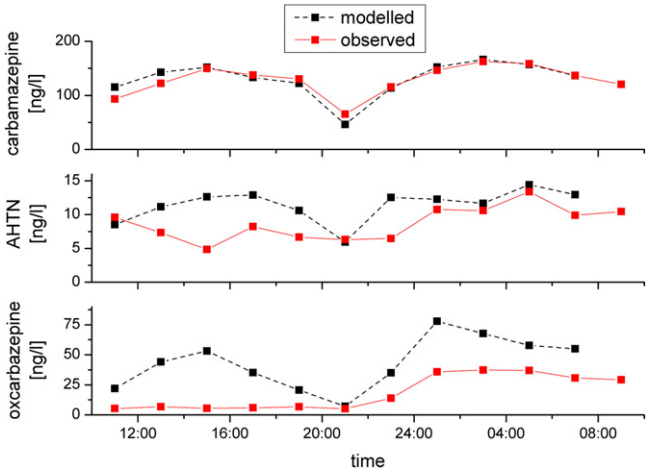

Fig. 6. Modeled and observed diurnal concentrations of selected micropollutants at the downstream end of the studied river segment.

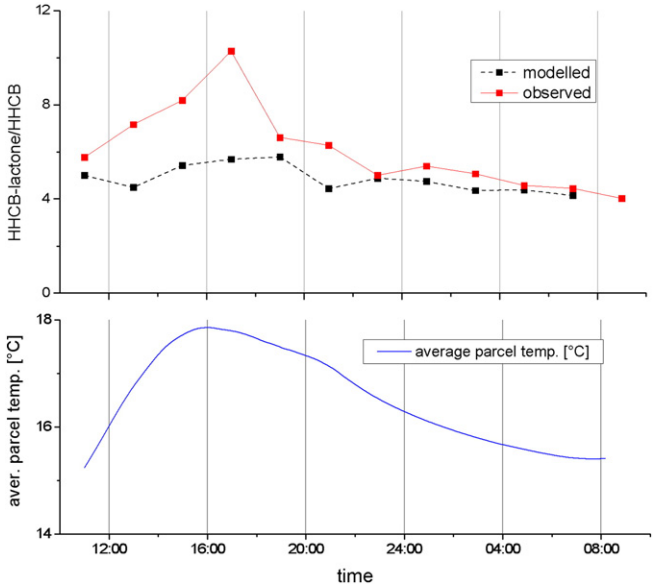

Fig. 7. Modeled and observed concentration ratios of HHCB-lactone/HHCB at the LCCS (top) and average water temperature experienced by each water parcel arriving at the LCCS (bottom).

river Ammer (Lange et al., 2015). However, it has to be taken into account that any further transformation of HHCB-lactone could mask degradation of HHCB. As a consequence, the more or less constant ratio of HHCB-lactone/HHCB during the night does not indicate that no further degradation occurs, but rather that relative transformation rates for both compounds are similar. In fact, the daily load of HHCB-lactone decreases along the river segment by net 3.1 g d^{-1} (Table 2), despite its production by degradation of HHCB. If the loss of 1.2 g d^{-1} HHCB is completely degraded to HHCB-lactone, up to 4,3 g d^{-1} HHCB-lactone is transformed which equals 25% of the input to the river segment (as opposed to net removal of 17.7% according to Table 2). In line with the other musk fragrances, the HHCB loss could as well partly be due to volatilization, peaking with maximum water temperatures in the afternoon hours (Fig. 7).

Further processes that may remove substances from the water column are sedimentation after sorption to particles (Schwientek et al., 2013) or direct sorption to the bed substrate. The former process is believed to be negligible in the studied case since observed turbidities were consistently below 2 NTU (nephelometric turbidity unit) corresponding to very low suspended solids concentrations of 2–3 mg L^{-1} (Rügner et al., 2014). In contrast, sorption to the bed substrate is a process that needs to be studied further. However, no clear correlation between net removal of studied compounds and their known octanol–water partitioning coefficients (Table 1) was observed. Therefore, it can be assumed that this physico-chemical property, and its associated mechanisms, did not play a major role.

4. Concluding remarks

The approach presented here was proven to be feasible for the determination of reliable mass balances and, ultimately, the site-specific reactivity of the selected representative micro-pollutants under given boundary conditions. The accuracy of the results is highlighted by the negligible removal of conservative tracers such as Cl^-, SO_4^{2-}, and Na^+. Furthermore, it was shown that a model-aided analysis of the bulk elimination rates as a function of time gives insights into the nature of processes and their temporal variability. The results also demonstrate that transformation of many micropollutants in rivers is highly variable in the course of a diurnal cycle. One of the main drivers of this variability is solar radiation that governs photo-oxidation. The importance of biodegradation was indicated by the occurrence of the intermediate HHCB-lactone and the changing HHCB-lactone/HHCB ratios over time. Changing water temperature may have an additional effect on the intensity of biologically and chemically (e.g. hydrolysis) mediated processes. Methods that capture snapshots in time will not account for these observed process dynamics. Such approaches are likely applied during the daytime and may miss reduced reaction rates during nighttime and, therefore, over-estimate transformation.

The method presented might be applied to comparative studies in rivers with contrasting characteristics (morphology, geochemistry) for the purpose of resolving the factors governing different transformation and elimination processes. Here, the creation of an extensive data base, covering diverse environmental conditions, could be a promising option to gain a better understanding of the transformation of micropollutants in rivers. This is of great importance as so far, many available studies which rely on less accurate quantification methods lead to ambiguous results. Moreover, the approach may be further developed in the future, e.g. by using more than two control cross-sections or by applying suitable tracer substances indicative of specific processes in order to improve the spatial and temporal resolution and to better distinguish different mechanisms and their rates. Finally, the role of sorption to the bed substrate and particle-facilitated transport may be an important area of further research.

Acknowledgments

This work was supported by a joint grant from the Helmholtz Center for Environmental Research, Leipzig (UFZ) and the Ministry of Science, Research and Arts of Baden-Württemberg (AZ Zu 33-721.3-2). The study was also supported by the EU FP7 Collaborative Project GLOBAQUA (Grant Agreement no 603629).

References

Ahel, M., Giger, W., Schaffner, C., 1994. Behaviour of alkylphenol polyethoxylate surfactants in the aquatic environment — II Occurrence and transformation in rivers. Water Res. 28, 1143–1152.
Andreozzi, R., Marotta, R., Pinto, G., Pollio, A., 2002. Carbamazepine in water: persistence in the environment, ozonation treatment and preliminary assessment on algal toxicity. Water Res. 36, 2869–2877.
Balk, F., Ford, R.A., 1999. Environmental risk assessment for the polycyclic musks AHTN and HHCB in the EU: I. Fate and exposure assessment. Toxicol. Lett. 111, 57–79.
Banjac, Z., Ginebreda, A., Kuzmanovic, M., Marcé, R., Nadal, M., Riera, J.M., Barceló, D., 2015. Emission factor estimation of ca. 160 emerging organic microcontaminants by inverse modeling in a Mediterranean river basin (Llobregat, NE Spain). Sci. Total Environ. 520, 241–252. http://dx.doi.org/10.1016/j.scitotenv.2015.03.055.
Barber, L.B., Antweiler, R.C., Flynn, J.L., Keefe, S.H., Kolpin, D.W., Roth, D.A., Schnoebelen, D.J., Taylor, H.E., Verplanck, P.L., 2011. Lagrangian mass-flow investigations of inorganic contaminants in wastewater-impacted streams. Environ. Sci. Technol. 45, 2575–2583. http://dx.doi.org/10.1021/es104138y.
Battaglin, W.A., Kendall, C., Chang, C.C.Y., Silva, S.R., Campbell, D.H., 2001. Chemical and isotopic evidence of nitrogen transformation in the Mississippi River, 1997–98. Hydrol. Process. 15, 1285–1300. http://dx.doi.org/10.1002/hyp.214.
Bester, K., 2004. Retention characteristics and balance assessment for two polycyclic musk fragrances (HHCB and AHTN) in a typical German sewage treatment plant. Chemosphere 57, 863–870. http://dx.doi.org/10.1016/j.chemosphere.2004.08.032.
Bester, K., 2005. Polycyclic musks in the Ruhr catchment area — transport, discharges of waste water, and transformations of HHCB, AHTN and HHCB-lactone. J. Environ. Monit. 7, 43–51. http://dx.doi.org/10.1039/b409213a.
Birgand, F., Skaggs, R.W., Chescheir, G.M., Gilliam, J.W., 2007. Nitrogen removal in streams of agricultural catchments — a literature review. Crit. Rev. Environ. Sci. Technol. 37, 381–487. http://dx.doi.org/10.1080/10643380600966426.
Brown, J.B., Battaglin, W.A., Zuellig, R.E., 2009. Lagrangian sampling for emerging contaminants through an urban stream corridor in Colorado. J. Am. Water Resour. Assoc. 45, 68–82. http://dx.doi.org/10.1111/j.1752-1688.2008.00290.x.
Buerge, I.J., Buser, H.-R., Müller, M.D., Poiger, T., 2003. Behavior of the polycyclic musks HHCB and AHTN in Lakes, two potential anthropogenic markers for domestic wastewater in surface waters. Environ. Sci. Technol. 37, 5636–5644.
Carmona, E., Andreu, V., Picó, Y., 2014. Occurrence of acidic pharmaceuticals and personal care products in Turia River Basin: from waste to drinking water. Sci. Total Environ. 484, 53–63. http://dx.doi.org/10.1016/j.scitotenv.2014.02.085.
Chen, X., Pauly, U., Rehfus, S., Bester, K., 2009. Personal care compounds in a reed bed sludge treatment system. Chemosphere 76, 1094–1101. http://dx.doi.org/10.1016/j.chemosphere.2009.04.023.
Cladière, M., Bonhomme, C., Vilmin, L., Gasperi, J., Flipo, N., Tassin, B., 2014. Modelling the fate of nonylphenolic compounds in the Seine River — part 1: determination of in-situ attenuation rate constants. Sci. Total Environ. 468–469, 1050–1058. http://dx.doi.org/10.1016/j.scitotenv.2013.09.028.
Clara, M., Strenn, B., Kreuzinger, N., 2004. Carbamazepine as a possible anthropogenic marker in the aquatic environment: investigations on the behaviour of Carbamazepine in wastewater treatment and during groundwater infiltration. Water Res. 38, 947–954. http://dx.doi.org/10.1016/j.watres.2003.10.058.
De Ridder, D.J., Verliefde, A.R.D., Heijman, S.G.J., Verberk, J.Q.J.C., Rietveld, L.C., van der Aa, L.T.J., Amy, G.L., van Dijk, J.C., 2011. Influence of natural organic matter on equilibrium adsorption of neutral and charged pharmaceuticals onto activated carbon. Water Sci. Technol. 63, 416–423. http://dx.doi.org/10.2166/wst.2011.237.
Deluchat, V., Lacour, S., Serpaud, B., Bollinger, J.-C., 2002. Washing powders and the environment: has TAED any influence on the complexing behaviour of phosphonic acids? Water Res. 36, 4301–4306. http://dx.doi.org/10.1016/S0043-1354(02)00160-4.
Dingman, S.L., 1984. Fluvial Hydrology. W.H. Freeman and Company, New York.
EPA, 2014. TSCA Work Plan Chemical Risk Assessment: HHCB. United States Environ. Prot. Agency (EPA Doc. 746-R1-4001).
Glassmeyer, S.T., Furlong, E.T., Kolpin, D.W., Cahill, J.D., Zaugg, S.D., Werner, S.L., Meyer, M.T., Kryak, D.D., 2005. Transport of chemical and microbial compounds from known wastewater discharges: potential for use as indicators of human fecal contamination. Environ. Sci. Technol. 39, 5157–5169. http://dx.doi.org/10.1021/es048120k.
Gómez, M.J., Martínez Bueno, M.J., Lacorte, S., Fernández-Alba, A.R., Agüera, A., 2007. Pilot survey monitoring pharmaceuticals and related compounds in a sewage treatment plant located on the Mediterranean coast. Chemosphere 66, 993–1002. http://dx.doi.org/10.1016/j.chemosphere.2006.07.051.
HERA, 2002. Targeted Risk Assessment of TAED. Hum. Environ. Risk Assess. ingredients Eur. Househ. Clean. Prod.
Ilchmann, A., Wienke, G., Meyer, T., Gmehling, J., 1993. Bestimmung von Verteilungskoeffizienten mit Hilfe der Flüssig/Flüssig-Gegenstrom-Chromatographie. Chem. Ing. Tech. 65, 72–75.
Jekel, M., Dott, W., Bergmann, A., Dünnbier, U., Gnirß, R., Haist-Gulde, B., Hamscher, G., Letzel, M., Licha, T., Lyko, S., Miehe, U., Sacher, F., Scheurer, M., Schmidt, C.K.,

Reemtsma, T., Ruhl, A.S., 2015. Selection of organic process and source indicator substances for the anthropogenically influenced water cycle. Chemosphere 125, 155–167. http://dx.doi.org/10.1016/j.chemosphere.2014.12.025.
Kasprzyk-Hordern, B., Dinsdale, R.M., Guwy, A.J., 2009. The removal of pharmaceuticals, personal care products, endocrine disruptors and illicit drugs during wastewater treatment and its impact on the quality of receiving waters. Water Res. 43, 363–380. http://dx.doi.org/10.1016/j.watres.2008.10.047.
Köck-Schulmeyer, M., Villagrasa, M., López de Alda, M., Céspedes-Sánchez, R., Ventura, F., Barceló, D., 2013. Occurrence and behavior of pesticides in wastewater treatment plants and their environmental impact. Sci. Total Environ. 458–460, 466–476. http://dx.doi.org/10.1016/j.scitotenv.2013.04.010.
Köhler, H.-R., Triebskorn, R., 2013. Wildlife ecotoxicology of pesticides: can we track effects to the population level and beyond? Science 341, 759–765.
Kunkel, U., Radke, M., 2011. Reactive tracer test to evaluate the fate of pharmaceuticals in rivers. Environ. Sci. Technol. 45, 6296–6302. http://dx.doi.org/10.1021/es104320n.
Lange, C., Kuch, B., Metzger, J.W., 2015. Occurrence and fate of synthetic musk fragrances in a small German river. J. Hazard. Mater. 282, 34–40. http://dx.doi.org/10.1016/j.jhazmat.2014.06.027.
Lester, Y., Sharpless, C.M., Mamane, H., Linden, K.G., 2013. Production of photo-oxidants by dissolved organic matter during UV water treatment. Environ. Sci. Technol. 47, 11726–11733.
Löffler, D., Römbke, J., Meller, M., Ternes, T.A., 2005. Environmental fate of pharmaceuticals in water/sediment systems. Environ. Sci. Technol. 39, 5209–5218.
Loos, R., Carvalho, R., António, D.C., Comero, S., Locoro, G., Tavazzi, S., Paracchini, B., Ghiani, M., Lettieri, T., Blaha, L., Jarosova, B., Voorspoels, S., Servaes, K., Haglund, P., Fick, J., Lindberg, R.H., Schwesig, D., Gawlik, B.M., 2013. EU-wide monitoring survey on emerging polar organic contaminants in wastewater treatment plant effluents. Water Res. 47, 6475–6487. http://dx.doi.org/10.1016/j.watres.2013.08.024.
Majewsky, M., Farlin, J., Bayerle, M., Gallé, T., 2013. A case-study on the accuracy of mass balances for xenobiotics in full-scale wastewater treatment plants. Environ. Sci. Processes Impacts 15, 730–738. http://dx.doi.org/10.1039/c3em30884g.
Maloszewski, P., 1993. Principles and practice of calibration and validation of mathematical models for the interpretation of environmental tracer data in aquifers. Adv. Water Resour. 16, 173–190.
Maloszewski, P., Zuber, A., 1982. Determining the turnover time of groundwater systems with the aid of environmental tracers, 1. Models and their applicability. J. Hydrol. 57, 207–231.
Matamoros, V., Nguyen, L.X., Arias, C.A., Salvadó, V., Brix, H., 2012. Evaluation of aquatic plants for removing polar microcontaminants: a microcosm experiment. Chemosphere 88, 1257–1264. http://dx.doi.org/10.1016/j.chemosphere.2012.04.004.
McGuire, K.J., McDonnell, J.J., 2006. A review and evaluation of catchment transit time modeling. J. Hydrol. 330, 543–563. http://dx.doi.org/10.1016/j.jhydrol.2006.04.020.
Meyer, J., Bester, K., 2004. Organophosphate flame retardants and plasticisers in wastewater treatment plants. J. Environ. Monit. 6, 599–605. http://dx.doi.org/10.1039/b403206c.
Moody, J.A., 1993. Evaluation of the Lagrangian Scheme for Sampling the Mississippi River during 1987–90. U.S. Geol. Surv.
Moody, R.P., Carroll, J.M., Kresta, A.M.E., 1987. Automated high performance liquid chromatography and liquid scintillation counting determination of pesticide mixture octanol/water partition rates. Toxicol. Ind. Health 3, 479–490.
Morrall, D., McAvoy, D., Schatowitz, B., Inauen, J., Jacob, M., Hauk, A., Eckhoff, W., 2004. A field study of triclosan loss rates in river water (Cibolo Creek, TX). Chemosphere 54, 653–660. http://dx.doi.org/10.1016/j.chemosphere.2003.08.002.
Musolff, A., Leschik, S., Möder, M., Strauch, G., Reinstorf, F., Schirmer, M., 2009. Temporal and spatial patterns of micropollutants in urban receiving waters. Environ. Pollut. 157, 3069–3077. http://dx.doi.org/10.1016/j.envpol.2009.05.037.
Nakada, N., Kiri, K., Shinohara, H., Harada, A., Kuroda, K., Takizawa, S., Takada, H., 2008. Evaluation of pharmaceuticals and personal care products as water-soluble molecular markers of sewage. Environ. Sci. Technol. 42, 6347–6353. http://dx.doi.org/10.1021/es7030856.
Pang, L., Liu, J., Yin, Y., Shen, M., 2013. Evaluating the sorption of organophosphate esters to different sourced humic acids and its effects on the toxicity to *Daphnia magna*. Environ. Toxicol. Chem. 32, 2755–2761. http://dx.doi.org/10.1002/etc.2360.
Reemtsma, T., Weiss, S., Mueller, J., Petrovic, M., Gonzales, S., Barcelo, D., Ventura, F., Knepper, T.P., 2006. Polar pollutants entry into the water cycle by municipal wastewater: A European perspective. Environ. Sci. Technol. 40, 5451–5458.
Regnery, J., Püttmann, W., 2010a. Occurrence and fate of organophosphorus flame retardants and plasticizers in urban and remote surface waters in Germany. Water Res. 44, 4097–4104. http://dx.doi.org/10.1016/j.watres.2010.05.024.
Regnery, J., Püttmann, W., 2010b. Seasonal fluctuations of organophosphate concentrations in precipitation and storm water runoff. Chemosphere 78, 958–964. http://dx.doi.org/10.1016/j.chemosphere.2009.12.027.
Rügner, H., Schwientek, M., Egner, M., Grathwohl, P., 2014. Monitoring of event-based mobilization of hydrophobic pollutants in rivers: calibration of turbidity as a proxy for particle facilitated transport in field and laboratory. Sci. Total Environ. 490, 191–198. http://dx.doi.org/10.1016/j.scitotenv.2014.04.110.
Sandstrom, Mark W., Kolpin, D.D.W., Thurman, M.E., Zaugg, S.D., 2005. Widespread detection of N,N-diethyl-m-toluamide in U.S. streams: comparison with concentrations of pesticides, personal care products, and other organic wastewater compounds. Environ. Toxicol. Chem. 24, 1029–1034.
Sasaki, K., Takeda, M., Uchiyama, M., 1981. Toxicity, absorption and elimination of phosphoric acid triesters by killifish and goldfish. Bull. Environ. Contam. Toxicol. 27, 775–782. http://dx.doi.org/10.1007/BF01611095.
Scheytt, T., Mersmann, P., Lindstädt, R., Heberer, T., 2005. 1-Octanol/water partition coefficients of 5 pharmaceuticals from human medical care: carbamazepine, clofibric acid, diclofenac, ibuprofen, and propyphenazone. Water Air Soil Pollut. 165, 3–11.
Schwientek, M., Rügner, H., Beckingham, B., Kuch, B., Grathwohl, P., 2013. Integrated monitoring of particle associated transport of PAHs in contrasting catchments. Environ. Pollut. 172, 155–162. http://dx.doi.org/10.1016/j.envpol.2012.09.004.
Simonich, S.L., Federle, T.W., Eckhoff, W.S., Rottiers, A., Webb, S., Sabaliunas, D., de Wolf, W., 2002. Removal of fragrance materials during U.S. and European wastewater treatment. Environ. Sci. Technol. 36, 2839–2847. http://dx.doi.org/10.1021/es025503e.
Ternes, T.A., 1998. Occurrence of drugs in German sewage treatment plants and rivers. Water Res. 32, 3245–3260.
Ternes, T.A., 2007. The occurrence of micopollutants in the aquatic environment: a new challenge for water management. Water Sci. Technol. 55, 327–332.
Ternes, T.A., Joss, A., Siegrist, H., 2004. Scrutinizing pharmaceuticals and personal care products in wastewater treatment. Environ. Sci. Technol. 38, 392A–399A.
Von der Ohe, P.C., Schmitt-Jansen, M., Slobodnik, J., Brack, W., 2012. Triclosan — the forgotten priority substance? Environ. Sci. Pollut. Res. 19, 585–591. http://dx.doi.org/10.1007/s11356-011-0580-7.
WHO, 1998. Environmental Health Criteria 209. Flame Retardants: tris(chloropropyl) phosphate and tris(2-chloroethyl) phosphate (Geneva).
Writer, J.H., Ryan, J.N., Keefe, S.H., Barber, L.B., 2012. Fate of 4-nonylphenol and 17 β-estradiol in the Redwood River of Minnesota. Environ. Sci. Technol. 46, 860–868. http://dx.doi.org/10.1021/es2031664.
Yang, X., Flowers, R.C., Weinberg, H.S., Singer, P.C., 2011. Occurrence and removal of pharmaceuticals and personal care products (PPCPs) in an advanced wastewater reclamation plant. Water Res. 45, 5218–5228. http://dx.doi.org/10.1016/j.watres.2011.07.026.
Yu-Chen Lin, A., Plumlee, M.H., Reinhard, M., 2006. Natural attenuation of pharmaceuticals and alkylphenol polyethoxylate metabolites during river transport: photochemical and biological transformation. Environ. Toxicol. Chem. 25, 1458–1464.
Zhang, Y., Geissen, S.-U., Gal, C., 2008. Carbamazepine and diclofenac: removal in wastewater treatment plants and occurrence in water bodies. Chemosphere 73, 1151–1161. http://dx.doi.org/10.1016/j.chemosphere.2008.07.086.
Zhang, X., Brar, S.K., Yan, S., Tyagi, R.D., Surampalli, R.Y., 2013. Fate and transport of fragrance materials in principal environmental sinks. Chemosphere 93, 857–869. http://dx.doi.org/10.1016/j.chemosphere.2013.05.055.